Metascintillators for Ultrafast Gamma Detectors: A Review of Current State and Future Perspectives

Georgios Konstantinou, Paul Lecoq, *Fellow, IEEE*, Jose M. Benlloch, and Antonio J. Gonzalez, *Member, IEEE*

***Abstract*—Scintillation detector development is an active field of research, especially for its application to the medical imaging field and in particular to the positron emission tomography (PET). Effective sensitivity and signal-to-noise ratio in PET are greatly enhanced when improving detector timing capabilities: the availability to provide time-of-flight (TOF) information. However, physical barriers related to the characteristics of available organic and inorganic scintillators create a trade-off between photon kinetics and gamma detection efficiency. We introduce the novel concept of metascintillators, composite topologies comprising of multiple scintillating and light-guiding materials functioning in synergy, that break this compromise. We provide an overview of published, ongoing and upcoming developments within this framework. Unconventional topologies, such as the multiple slabs approach comprising of a high-Z host and a fast emitter; materials such as CdSe/CdS nanoplatelets; and treatments related to nanostructured metamaterials and photonic interactions, are reviewed and complemented with new, unpublished advances in simulations and analysis. Future perspectives are further presented, encompassing developments in signal analysis and system integration. Within this concept, an improved generation of detectors and PET scanners with unprecedented time resolution is researched, paving the way toward the 10-ps TOF PET challenge for the advancement of PET and improvement of public health.**

***Index Terms*—Positron emission tomography (PET), radiation detectors, scintillators, time of flight (TOF).**

I. Introduction

A. Time of Flight

IN POSITRON emission tomography (PET) and related applications, one can denote an increasing demand for PET examinations [1], curtailed only by the techno-economical, engineering, and physical limitations of the process. While nothing can be done for the latter, and the first is out of the scope of academic discussion, PET instrumentation and image reconstruction developments remain very active fields. In the last years, new solutions in both hardware and software have resulted in significant improvements in effective sensitivity [2], [3].

Manuscript received October 23, 2020; revised January 29, 2021 and February 25, 2021; accepted March 16, 2021. Date of publication April 2, 2021; date of current version December 30, 2021. This work was supported in part by the European Research Council (ERC) under the European Union's Horizon 2020 Research and Innovation Program under Grant 695536: 4D-PET. *(Corresponding author: Georgios Konstantinou.)*

Georgios Konstantinou is with Multiwave Metacrystal S.A., 1228 Geneva, Switzerland (e-mail: georgios@metacrystal.ch).

Paul Lecoq is with Multiwave Metacrystal S.A., 1228 Geneva, Switzerland, and also with the Instituto de Instrumentacion Imagen Molecular, CSIC-Universitat Politecnica de Valencia, 46022 Valencia, Spain.

Jose M. Benlloch and Antonio J. Gonzalez are with the Instituto de Instrumentacion Imagen Molecular, CSIC-Universitat Politecnica de Valencia, 46022 Valencia, Spain.

Color versions of one or more figures in this article are available at https://doi.org/10.1109/TRPMS.2021.3069624.

Digital Object Identifier 10.1109/TRPMS.2021.3069624

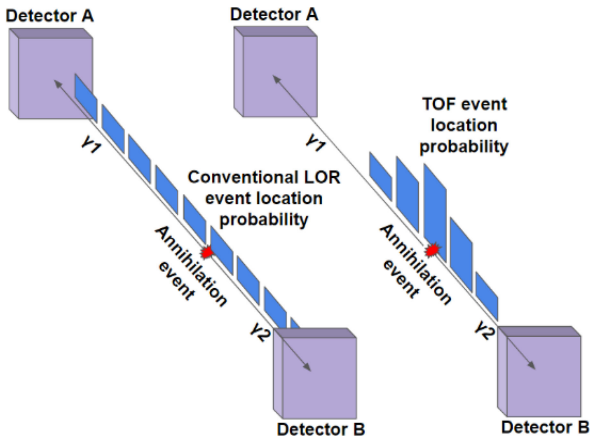

Fig. 1. Advantage of ToF in a nutshell: precise timing information qualify an area around the actual annihilation event epicenter as more probable for its reconstruction, retrieving enhanced information from each coincidence detection.

One way to increase the effective sensitivity is achieved by developing gamma detectors based on faster scintillators [4]. This relates to the potential of adding time-of-flight (TOF) information on the event characterization. TOF is the time necessary for the electron–positron annihilation produced gammas to be detected. As described in detail in the literature, TOF adds longitudinal information to the traditional line of response, allowing one for a more precise localization of the annihilation process (Fig. 1).

In particular, the time difference (Δt) between the two recorded timings (timestamps) of a coincidence pair corresponds to a Δx distance according to [5]

$$\Delta t = \frac{2\Delta x}{c} \tag{1}$$

where c is the speed of light in a vacuum. Without TOF, the number of resolution cells equals the number of voxels along the line of response. Having access to TOF information reduces the effective number of resolution elements. The reduction through TOF improves the statistical properties of the PET image and leads to an improvement of the signal-to-noise ratio (SNR) for the same amount of information and

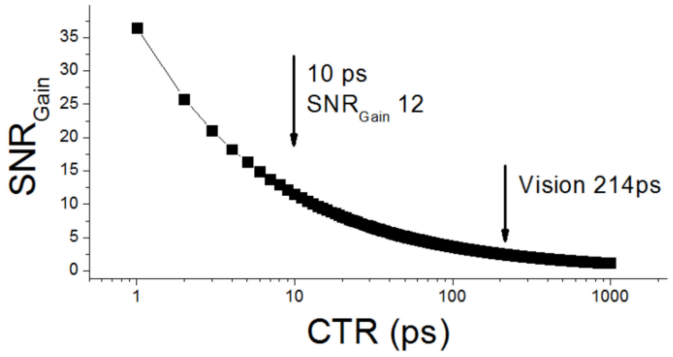

Fig. 2. SNR gain by the improvement of detector ToF resolution. Vision 214 ps corresponds to the best existing commercial model ToF resolution [6].

acquisition time, as quantified in

$$\frac{\mathrm{SNR_{TOF}}}{\mathrm{SNR_{PET}}} = \sqrt{\frac{D}{\Delta x}} = \sqrt{\frac{2D}{c\Delta t}} \tag{2}$$

where D is the diameter of the object to be imaged. Timing in the range of 200-ps FWHM, the current state of the art for commercial designs set by the Siemens Biograph Vision [6] leads to only 3-cm position uncertainty in the longitudinal direction. In this case, in a human brain with a 20-cm diameter, the TOF SNR improvement is close to 3. A coincidence timing resolution (CTR) of 10 ps leads to 1.5-mm TOF information, corresponding to an improvement of 12 (Fig. 2). This spatial TOF resolution approaches the physical limit of positron range [7] and is similar to the standard voxel dimensions of existing scanners. This might allow for virtually reconstruction-less acquisitions and a quantum leap in detector effective sensitivity [8], leading to an important reduction of radiotracer dose and examination duration. With such coincidence timing and corresponding sensitivity improvement, PET technology gains an unprecedented advantage in the nascent fields of molecular imaging and theranostics [9].

B. PET Detectors

The gamma detector block in a PET scanner is based on the physical process of scintillation. This is the characteristic property of particular materials able of capturing an incoming high-energy gamma ray and release part of its energy in a shower of lower energy optical photons. These scintillation photons are detected by photosensors such as silicon photomultipliers (SiPMs), capable of producing a measurable electric signal. This signal is then digitized, allowing the registration of the main characteristics of the optical shower, such as the time of arrival and total energy.

Recent developments in PET instrumentation include very fast SiPM [10] that can be read out by sub-10-ps time-to-digital converters (TDCs) [11]. These advances have a high technological readiness level, meaning that they will soon be deployable in an industrial scale. However, the physical process of scintillation currently constitutes the bottleneck in the quest for ultrafast gamma detectors. The speed of transformation of an incoming gamma to a measurable shower of low-energy photons is key for the accurate timing characterization of the events. This depends exclusively on the type of scintillator.

C. Scintillation

Scintillation is the process in which a material converts the energy of an incident particle (UV, X-ray, or γ-ray) into a number of photons of much lower energy, in the visible or near-visible range, which can be easily detected with current photomultipliers, photodiodes, or avalanche photodiodes [12]. There exist two main scintillator categories, namely, organic and inorganic, that work through different mechanisms. Nevertheless, for a material to be a scintillator, it must contain luminescent centers, which are activated by the incoming ionization radiation.

The time function of optical photon production through this multistep process is accurately modeled through the biexponential model shown in (3), where E is the gamma energy, LY_{scint} is the light yield, and τ_{rise} and τ_{decay} correspond to rise and decay times, respectively [13]

$$f_{\mathrm{scint}}(t) = \frac{E \times LY_{\mathrm{scint}}}{\tau_{\mathrm{decay}} - \tau_{\mathrm{rise}}} \left(e^{-\frac{t}{\tau_{\mathrm{decay}}}} - e^{-\frac{t}{\tau_{\mathrm{rise}}}} \right). \tag{3}$$

D. Scintillators

Since its development, lutetium–yttrium oxyorthosilicate (LYSO) has taken the lead from bismuth germanium oxide (BGO) as the golden standard for scintillation-based detectors, due to its favorable optical photon production kinetics. Both LYSO and BGO are inorganic scintillators. They are well suited for PET due to their high effective atomic number (high-Z) and density, which correspond to high photoelectric cross section and hence stopping power for the 511-keV annihilation gammas. LYSO has a very fast response, with a rising exponential of 74 ps and a decay one of around 40 ns, in the biexponential model. It produces a large yield of optical photons (around 32 000 per MeV) and has a large absorption length for the wavelengths of emission, both factors improving timing capabilities [14]. There is still a wide variety of scintillation materials available [8] with potential application for TOF PET. Also in the inorganic domain, barium fluoride (BaF_2) has the remarkable capability of producing two independent pulses [15]. Its fast decay component has a duration of only 600–800 ps producing about 1800 optical photons per MeV in the V-UV range. This fast pulse can provide better timing than LYSO, at the cost of lower stopping power (density).

Scintillating materials expand beyond the realm of inorganic crystals. In particular, plastic scintillators, produced commercially by various companies in patented designs [16] often provide fast kinetics with sufficient light yield. As an example, Eljen's EJ232 produces 8400 optical photons with a 350-ps rise and 1.4-ns decay times, respectively. The reason that such components are not more broadly used for the TOF PET application comes from their low density that significantly reduces their stopping power for energetic gamma rays. Nevertheless, a whole-body PET design exclusively based on plastic scintillators has been developed [17]. This design compensates its

low detection efficiency with an accurate TOF resolution of 266 ps, and a very long axial field of view (FoV). Similarly, modern developments of perovskite scintillators could lead to improved scintillating characteristics, even though these compounds are still in the research phase and often require particular conditions such as very low temperature [18].

Furthermore, when making use of thick scintillators, there are more possible paths for a photon to travel before reaching the photon detector, leading to the increased variance of time delays [19]. This uncertainty is detrimental for fast timing on the picosecond scale. This is clearly demonstrated by the estimation of the statistical lower bound, calculated through the Cramér–Rao method [20]. This statistical measure corresponds to the number of photons that have to be detected within a given time in order to define the time of a scintillation event.

In short, the tradeoff between detector material, elementary detector size, and timing resolution seems to be unbreakable with conventional scintillator solutions. The purpose of this article is to introduce the novel concept of metascintillators, which intends to address this tradeoff.

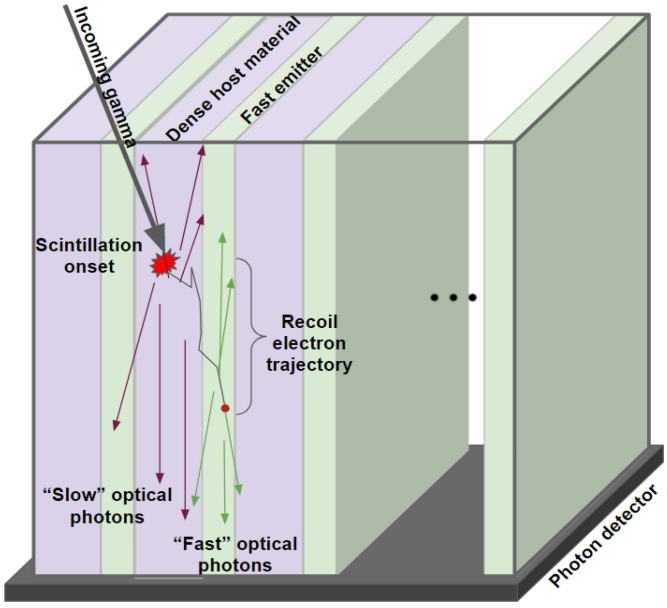

Fig. 3. Example of a metascintillator topology: thin slices of a dense host material and a fast emitter are placed next to each other, allowing scintillation production in both.

E. Definition of Metascintillators

In material science, the concept of metamaterials was theorized by the physicist Victor Veselago in 1968 [21] for the particular application of materials with a negative refraction index. Since then, this meaning has expanded to suggest any synthetic composite material with a structure such that it exhibits properties not usually found in natural materials [22]. Concerning scintillators, we could define as metascintillators the composite topologies of scintillating and light-guiding materials, arranged to produce a synergistic effect at some step of the scintillation process, from gamma absorption to light detection, combining thus the favorable physical characteristics of their constituting components. The efforts in this direction are intended to provide the basis for future developments that can lead to TOF PET with sufficient gamma detection efficiency combined with a timing resolution in the order of 10 ps over the next years [23].

The two fundamental mechanisms of electromagnetic interactions relevant in PET instrumentation are photoabsorption and Compton scattering. In both cases, a recoil electron is produced at the beginning of the gamma interaction. The recoil electron is interacting with the scintillator all along its travel path, losing energy through a *dE/dx* process that leads to the generation of electrons and holes that can directly excite the luminescent centers or bind together in so-called excitons. The excitons can directly recombine radiatively or be trapped by luminescent centers or impurities boosting or quenching the luminescence. The travel range of the recoil electron depends on the intrinsic characteristics of the scintillating medium with a strong correlation to its density. For dense organic scintillators, the recoil electron range reaches up to around 500 μm.

One way to combine the favorable characteristics of different scintillators is to have different scintillators sharing the energy of a gamma interaction. Notice that in principle there are no mechanisms to confine the recoil electron within a particular medium. This means that different scintillating materials, if placed in close proximity, can share the optical photon production related to a single interacting annihilation gamma. Hence, it is possible to use a high-Z material benefiting from its stopping power, and design a geometrical topology that brings fast optical photon emitters close enough, resulting in a substantial probability of recoil electrons crossing through them. Thus, some optical photons will be produced according to the favorable kinetics of the second material. Based on this concept, the first generation of composite metastructures includes a high-Z host and a fast emitter, cut in layers with thicknesses of less than the recoil electron range and arranged in geometrically periodic alternating positions (Fig. 3).

In the following sections, published works, including an experimental demonstration with different materials, are reviewed. These aim at better illustrating the claims made concerning the different sections. Also, detailed simulation analysis is provided, which demonstrates how the metascintillator can comprise a large family of combinatory metastructures designed for specific characteristics.

II. Metascintillators: Review of State of the Art

A. Plastic-Based Metascintillators

This simple approach has been tested and proof-of-concept results published in [24]. Both LYSO and BGO for their high-Z and the BC-422 plastic (Saint Gobain, France) as fast emitter were tested. This plastic has similar timing characteristics to the EJ232. A so-called metapixel was constructed by eight pairs of $3 \times 3 \times 0.25$ mm^3 BC-422 and $3 \times 3 \times 0.2$ mm^3 dense host, with a final dimension of $3 \times 3 \times 3.6$ mm^3. As expected for a pixel of such a small size and with such a high proportion of light material, the majority of interactions had

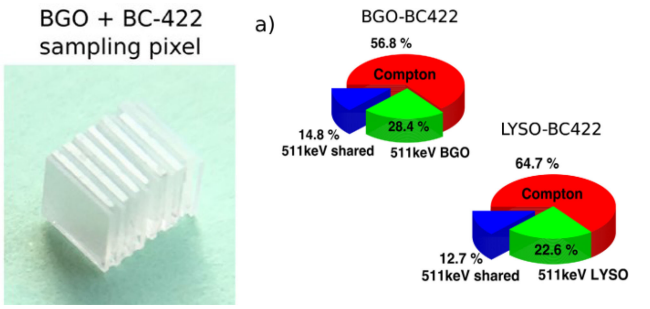

Fig. 4. (Left) Picture of a BGO-BC422 metascintillator pixel; and (right) BGO-BC422 and LYSO-BC422 interaction percentages. Figure taken from [24].

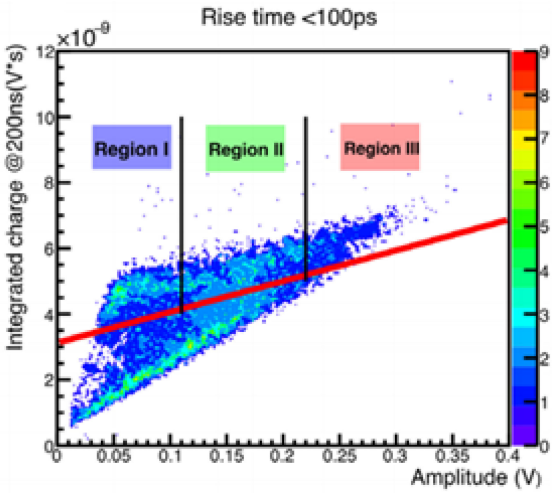

Fig. 5. Event distribution in a plot of 200-ns integral over maximum pulse amplitude for events with faster rise time, occurring due to event energy sharing. Figure taken from [24].

some energy leaking out of the pixel (Fig. 4). However, for the rest of interactions, a particular percentage of events was shared between the two materials, providing the first proof of concept for metascintillators.

Given that the light yields for BGO and BC-422 are similar, it is possible to detect the extent of energy sharing by comparing the pulse amplitude and the integral of the first 200 ps. As depicted in Fig. 5, this demonstrates a continuous form of energy sharing, from events purely taking place in BGO, constituting the majority of such interactions, to a smaller number of events mostly interacting with the plastic scintillator. The nature of sharing is important, as in order to detect the timing of such a metastructure precisely, it is paramount to know which scintillation mechanism led to the generation of photons. This way, the timing reconstruction algorithm will not only take into account information of, e.g., time walk [25], but it will be possible to estimate the scintillation event onset with higher precision, significantly improving the CTR.

Using such insight, in [24], the timing of different regions of energy sharing is calculated. BGO events lead to a 120-ps FWHM resolution, while the events with higher participation of the fast emitter reach as low as 40-ps FWHM. This proof of concept constitutes the first demonstration of energy sharing. Nevertheless, it was performed with a very small

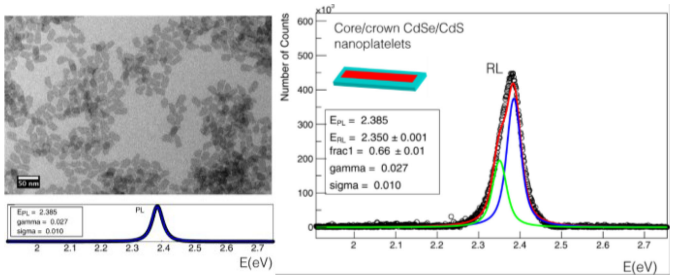

Fig. 6. Event distribution in a plot of 200-ns integral over maximum pulse amplitude (left) for all events and (right) for events with faster rise time, occurring due to event energy sharing. Figure taken from [26].

pixel. Pixel dimensions, as well as the mixture of different materials, surface treatment of slabs and light collection can have a high impact on the final specifications of metascintillators. Furthermore, different orientations of slab positioning should also be researched. Finally, this scheme can be further upgraded with the use of different types of scintillating components, such as for instance nanocrystals.

B. Nanocrystal-Based Metascintillators

Metascintillators can include any scintillating approach, to enhance their timing capabilities. Nanocrystals in particular, exhibit very fast scintillation properties if their size is smaller than the Bohr radius (∼10 nm) of the excitons, increasing their recombination rate because of this quantum confinement. For instance, CdSe nanocrystals stand out for their unparalleled timing performance and other advantages if produced in the form of nanoplatelets, confining the excitons in one direction only, and allowing even faster multiexciton recombinations [26]. They have been among the first direct band-gap semiconductor nanocrystals studied for the purpose of ultrafast timing detector applications. Their red-shifted radioluminescence signal demonstrating prompt (20 ps) photon production and a subnanosecond pulse duration makes them potential candidates for a new generation of metascintillators. However, their implementation as radiation detectors is technologically challenging owing to intrinsic shortcomings such as high self-absorption and the necessary presence of organic ligands needed for surface passivation and shaping the luminescence and spatial distribution of nanoplatelets.

CdSe nanoplatelets have been studied in a metascintillator configuration [26], where a high-Z material (LYSO) is used as the dense host providing its high detection efficiency. The excitons that reach through it the nanoplatelets then generate fast photons. In particular, CdSe/CdS core–crown nanoplatelets (Fig. 6) were studied in combination with state-of-the-art bulk materials such as LYSO, forming drop-casted films, or after an embedding procedure that uses polystyrene as a host matrix. In the first case, the combination of produced light and its timing characteristics were measured with the pioneer use of a streak camera (Hamamatsu Photonics, Japan) in an X-ray-induced radioluminescence experiment (see Fig. 7). An X-ray triggers the process of reading out the light from a sample over a range of wavelengths, providing unprecedented understanding of the physical process and light output.

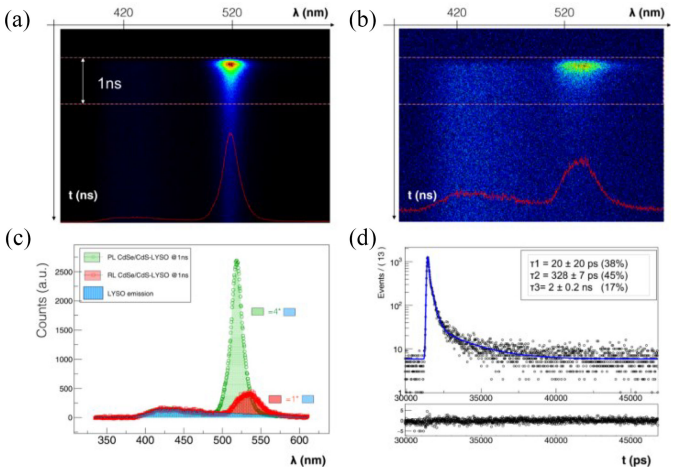

Fig. 7. (a) Photoluminescence and (b) radioluminescence time-resolved spectra of a CdSe/CdS drop-casted film deposited on an LYSO:Ce substrate as readout by a Hamamatsu streak camera. (c) Comparison of photoluminescence (green), radioluminescence (red), and LYSO emission (blue) wavelengths, integrated over the first nanosecond. (d) Time-resolved CdSe/CdS core–crown radioluminescence integrated from 200 to 800 nm as measured with a hybrid PMT in time-correlated single-photon counting mode. Figure taken from [26].

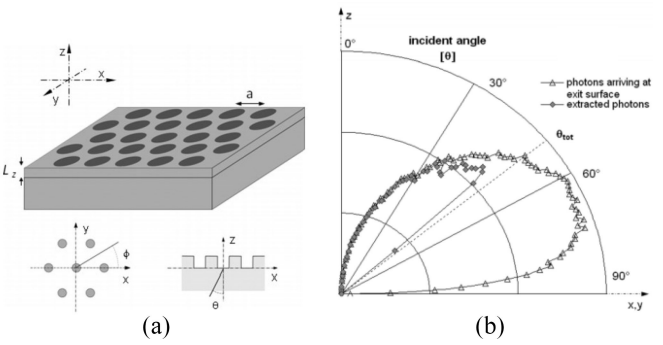

Fig. 8. Initial photonic crystal slab approaches: precise shape and arrangement of the nanostructured slab (a), increases the photon extraction efficiency beyond geometrical expectations (b).

The spectral time-resolved characterization of the metastructure demonstrates how CdSe/CdS light is collected in the first few hundreds of picoseconds after event onset. This corresponds to an extremely fast, practically prompt, mode of emission, denoting the very desirable timing characteristics of core–crown nanoplatelets drop casted on LYSO.

The optimal implementation of CdSe in a metacrystal heterostructure still needs to be studied in detail, due to a number of considerations concerning CdSe casing, concentration, and arrangement within the metascintillator. However, the strong and ultrafast pulse at a wavelength within specifications of most commercial SiPMs make them a candidate for next-generation metascintillator-based detectors.

C. Metamaterial Aspect of Metascintillators

The special property of electromagnetic metamaterials is usually obtained from the constructive and destructive interference of incoming light after scattering via a large number of periodic structurations. As the size of elements reaches dimensions in the same order of magnitude as the light wavelength, interactions are modeled more accurately through the wave model of light and Maxwell equations rather than the particle model of photons. In these conditions, with quantum effects gaining a dominant role, unusual properties can be found, such as negative refractive index, control of the direction of propagation, the possibility of gating, and perfect antireflection at all angles, among others [27].

Those optical phenomena could provide solutions to various challenges resulting from suboptimal light creation, propagation, and extraction in the scintillation paradigm. In particular, the isotropic character of scintillation light along with the high refraction index of most scintillators, play a pivotal role in the deterioration of time resolution on light detection. Efficient light collection improves the statistical probability of fast photons being registered, while directionality of light reduces the variance of optical paths, further enhancing single-detector time resolution. Such treatments fall within the framework of nanomanufacturing and nanophotonics, expanding in this way the multidisciplinary nature of metascintillator research. Developed photonic crystal slabs are thin layers of dielectric modulated by periodically varying permittivity or permeability, so to create multiscattering effects with lights.

Previous works focused a lot on improving light extraction efficiency [28]. Due to the high refractive index of crystal scintillators in their emission spectrum, total internal reflection (TIR) is the main optical propagation mechanism. This means that the probability of reaching the extraction side of the scintillator, where a photosensor is placed, in an angle that allows direct extraction is small and a significant percentage of photons, up to 90% in the case of BGO are reflected back. The majority of unextracted photons keep traveling within the optical medium, resulting in deterioration of timing resolution and increasing the probability of being absorbed. In this work, one layer of photonic crystal slab inserted between the scintillation crystal and the photon detector demonstrated that it is possible to fine-tune the pattern and optimize the light extraction (Fig. 8). With a simple periodic pattern, the simulation showed that for a significantly broader range of incident angles, photons would be extracted directly. Avoiding TIR has the potential to improve event SNR, energy resolution, and single-detector timing resolution.

This approach was further investigated through a laser-based experiment [29], where a green laser targets the extraction surface of an LYSO crystal, layered with a photonic slab (Fig. 9). By simulating scintillation light with this experiment, it is demonstrated that diffraction orders are generated at larger angles than allowed by the Snell law, depending on the characteristics of the photonic crystal slab pattern.

A set of scintillators treated with the addition of a photonic crystal slab at their read-out side were developed and tested (Fig. 10) [30]. The first experiment concerned a single-detector setup using 662 keV gammas from Cs-137. Most importantly, an ultrafast setup was used for coincidence experiments. This experiment demonstrated a significant improvement in both CTR (up to 57%) and light yield (up to 144%), providing

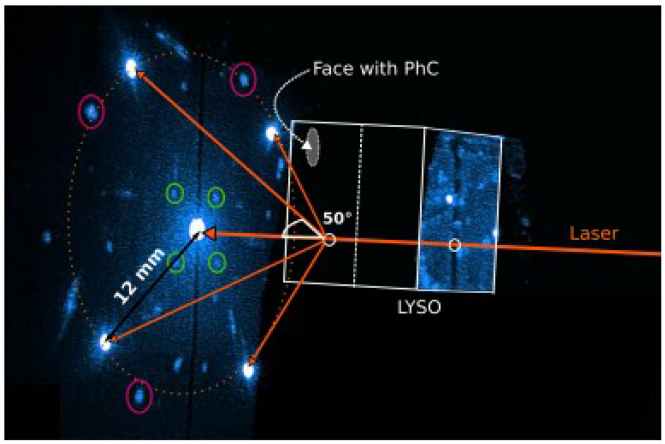

Fig. 9. Experiment performed on an LYSO crystal with the PhC slab pattern on the readout face. A green laser is used to simulate light, traveling inside the crystal, and interacting with the PhC slab from the inside. Diffraction orders are generated at an angle dependent on the periodicity of the pattern. The image is shown in false color to increase contrast. Figure taken from [29].

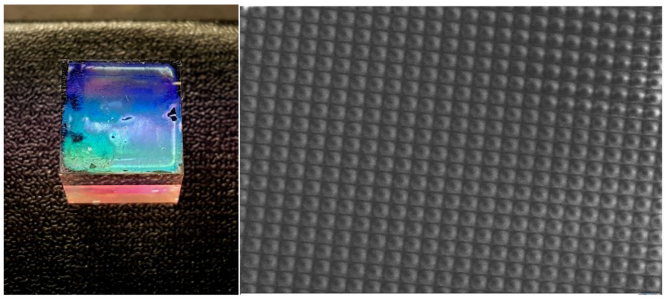

Fig. 10. (Left) Patterned sample with pattern facing up, showing diffraction colors; and (right) image of the patterned polymer on the read out face of a sample. Figure taken from [30].

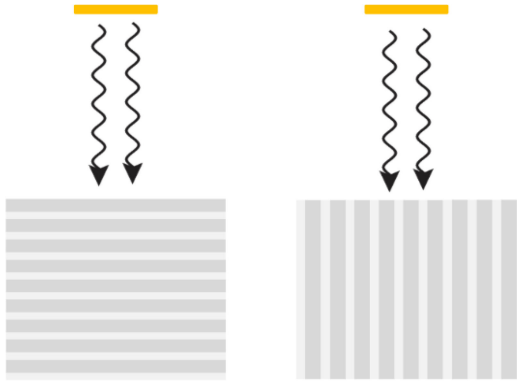

Fig. 11. Two simulated configurations of the simple metascintillator approach, for various slab thicknesses: (left) perpendicular and (right) parallel to the gamma direction.

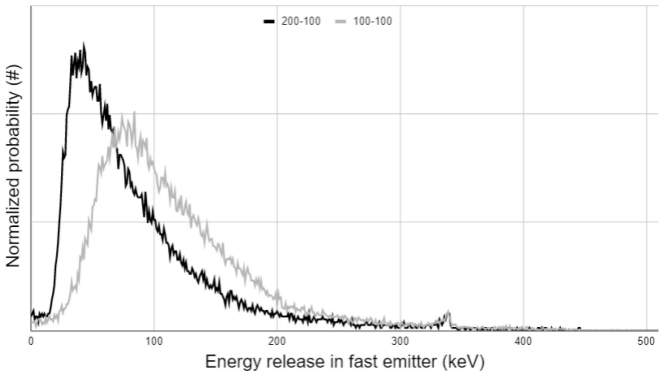

Fig. 12. Probability distribution of energy sharing (energy release in fast emitter) as resulting from simulations of two LYSO-EJ232 (200–100 um and 100–100 um, respectively) metascintillator scenarios.

a proof of concept for further research and development in this direction.

The concept of metascintillators can thus include a metamaterial aspect, when the metastructure includes layers that alter the direction of light in a nonclassical manner, in order to enhance scintillator detector efficiency. However, metascintillators as a concept are not based on metamaterial behavior, as energy sharing results from a different mechanism than those affecting light propagation in metamaterials.

D. Metascintillator Geometry

The dependence of metascintillator energy sharing on geometrical characteristics is a significant element to guide the choice of materials for further testing. This has been the main development direction presented in [31]. In order to estimate this, we run Monte Carlo simulations, using the GEANT4-based GATE software [32]. We used plastic as the fast emitter due to the existence of prior experimental results. Two distinct configurations of slabs oriented in parallel or perpendicularly to the gamma trajectory have been considered (Fig. 11), for slab thicknesses ranging from 50 to 300 μm. A number of materials have been considered for the role of the dense host, in particular, BGO, LYSO, and BaF_2. Detailed experimental results will be presented soon, however, the main insight provided by this exercise is briefly discussed in the following.

The probability for a particular percentage of energy to be deposited in the fast emitter, for each event, has been determined. This probability follows a distribution of a positively skewed normal character, compared to the energy deposited in the fast emitter material, as shown in Fig. 12. The general form of sharing is the same, however, differences in material and geometry slightly alter the average and deviation of this shape. A set of metrics to describe the quality of energy sharing and its applicability for gamma-ray detector development has been constructed. In particular, we calculated the average energy deposited in plastic, corresponding to the mean value of the distribution; the percentage of shared events among all events, following the approach in [24]. Most importantly, the percentage of events that can produce a significant number of fast photons, to allow for the determination of event onset timing through fast emitter kinetics was also computed. In the case of plastic-based metascintillators, we set this at 80 keV, about 15% for 511 keV events, corresponding to about 700 fast optical photons produced.

We found a very strong dependence between all these metrics and, the volume and mass percentage of the fast emitter

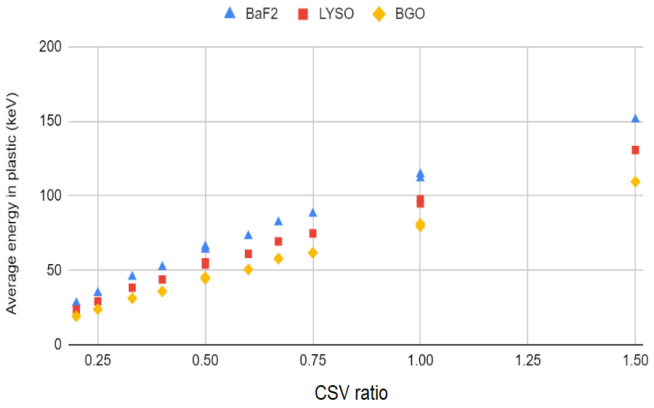

Fig. 13. Average energy in crystal as a function of CSV ratio for three different high-Z hosts (BaF2, LYSO, and BGO) and EJ232.

with respect to the dense host, which is named composing scintillation volume (CSV, Fig. 13) and mass (CSM) ratios.

While a higher CSV ratio demonstrates better photon kinetics, including a lot of the fast emitter (of low density and photoelectric cross section) in the design leads to a reduction in gamma detection efficiency. As Fig. 14 depicts, the average energy deposited in plastic has an exponential dependence with density (surrogate for detector efficiency). In order to evaluate the available scenarios, a qualitative approach, including light production and propagation of light, corresponding directly to anticipated timing characteristics of the metascintillator has to be devised.

E. Metascintillator Light Production Form

In the same work [31], some insight more has been given on the actual signal form resulting from metascintillator energy sharing. The photon production time-dependent effect follows energy sharing and thus varies for each event. In particular, the combination of scintillating characteristics of different materials leads to a new, double biexponential model, described in (4), where E_{int} corresponds to total gamma ray interaction energy and variables with f subscript correspond to the fast emitter, while s to the dense host

$$f_{\text{metascint}}(t) = \frac{E_f \times LY_f}{\tau_{fd} - \tau_{fr}}\left(e^{-\frac{t}{\tau_{fd}}} - e^{-\frac{t}{\tau_{fr}}}\right) + \frac{(E_{\text{int}} - E_f) \times LY_s}{\tau_{sd} - \tau_{sr}}\left(e^{-\frac{t}{\tau_{sd}}} - e^{-\frac{t}{\tau_{sr}}}\right). \quad (4)$$

Experience with such a multiexponential form has grown through scintillators such as BaF_2 [15]. In general, increasing variability of luminescent centers complicates the model, adding more biexponential factors. Moreover, metascintillators including BaF_2 have to be analyzed using a triple biexponential model. In order to further understand the effect of energy sharing in detector timing resolution, in Fig. 15, we present the form of the multiexponential models for LYSO, BGO, and BaF_2 combined with EJ232, for the two extremes of pure 511-keV crystal and plastic events, and for the case of 80 keV deposited in EJ232.

From this analysis, we observe that even for only 80-keV gamma energy being deposited in the fast emitter, the rising edge is already visibly improved, even for the case of highly luminous LYSO. This is the most difficult case, given the steep rising edge and high light yield of LYSO. In Fig. 16, the same pulse shapes are shown for LYSO combined with EJ232 as well as with CdSe nanoplatelets, as a reference of the effect a fast scintillator with lower light yield but shorter pulse can have to the rising edge of the metascintillator. The case of LYSO is focused on, as this crystal already provides a large amount of fast photons. Fig. 16 demonstrates how the addition of fast emitters significantly improves photon production within the first 200 ps after event onset.

To be able to estimate the photon contribution of the fast emitter that provides better timing resolution for highly shared events, there is the need to develop an algorithm. This way, it will be possible to calculate automatically both event energy as a whole as well as the contribution of the fast emitter. The continuous energy sharing probability distribution can be separated in a number of event regions, as shown in Fig. 5.

The pulse shape is characteristic of the constituting materials and their kinetics. The probability of a particular energy sharing depends on the geometrical and topological characteristics of the metascintillator. Moreover, this model only relates to optical photon production. Propagation and collection add extra factors that affect pulse shape and are predominantly dependent on optical space geometry and read-out architecture, among others. For the case of the addition of photonic crystal slabs, photon production will not be affected. Photon collection is greatly impacted though, depending on the geometry and efficiency of the slabs.

III. Future Perspectives

A. Cramér–Rao Lower Bound for Metascintillators

Scintillation kinetics play a major role in the detector timing resolution, as a faster material produces more optical photons within the first few picoseconds, that carry the timing information of event onset. Nevertheless, the propagation of photons affects the fidelity of retrieval of this information. A metascintillator design adds another condition, which is the event-specific percentage of energy sharing. This leads to a system that follows a combination of the fast emitter and the slower dense host photon production statistics. This means that the event onset timing of some events can be estimated through the timing precision provided by plastic scintillators, while the rest follows the standard crystal timing.

Another factor relates to the size and geometry of scintillator volume that is optically connected, allowing photons to traverse unhindered. This dictates the variability of paths that a photon can travel and the amount of photons to be absorbed before detection. This adds a statistical variation to the amount of photons collected at any given point of time.

In plastic-based metascintillator design, the overall density is lowered, leading to reduced gamma detection efficiency. In order to keep a high gamma detection efficiency, longer crystals can be considered. In particular, for a scenario based on LYSO slabs of 200-um thickness and EJ232 slabs of 100-ps

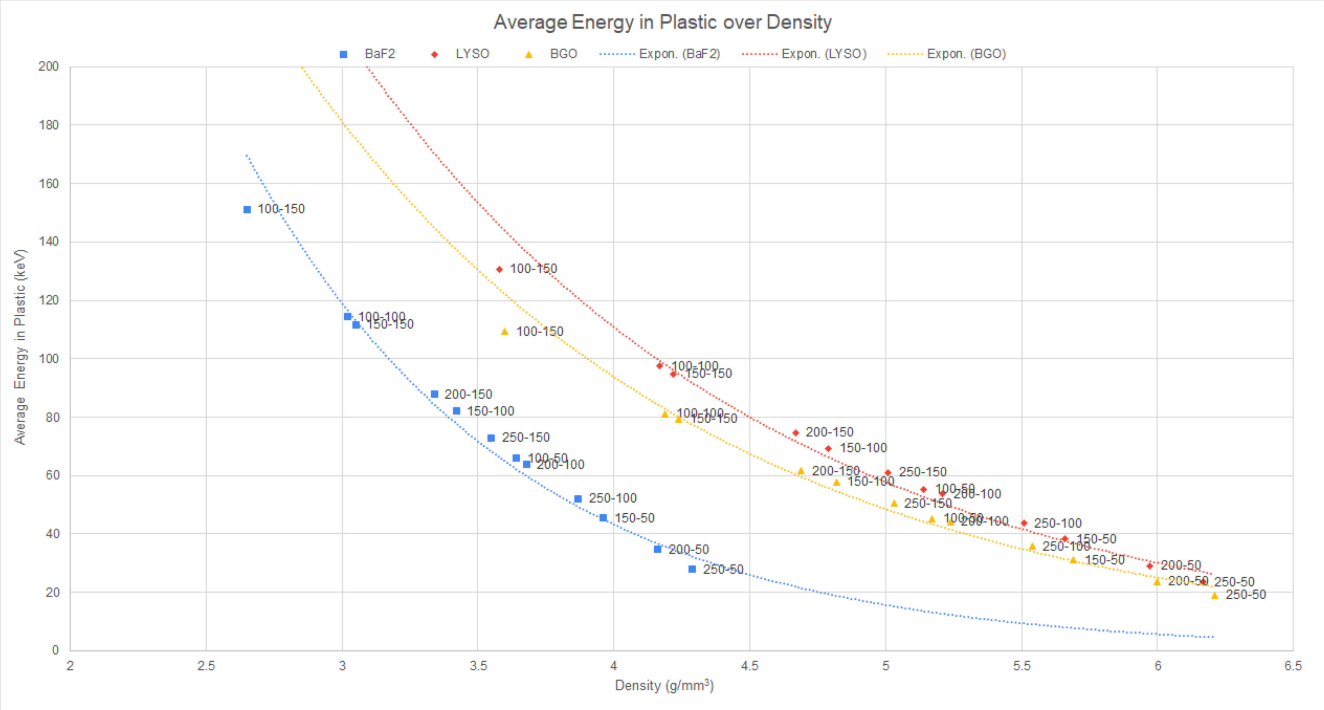

Fig. 14. Combinatory plot of all metascintillator combinations simulated, along with the exponential fit. Points are described by their crystal-plastic thicknesses and demonstrate the tradeoff between average event energy sharing and metascintillator density.

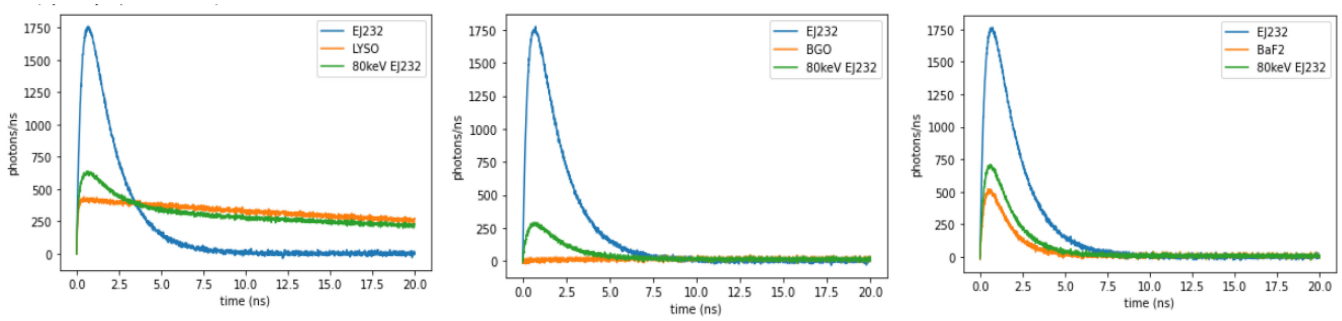

Fig. 15. 20-ns profile of plastic (EJ232)-based metascintillators, with (left) LYSO, (middle) BGO, and (right) BaF2 host crystal, for three different energy (0, 80, and 511 keV in plastic) contents.

thickness, in order to achieve the same gamma detection efficiency as Siemens Biograph Vision [6], crystal length needs to be expanded from 20 to 27 mm. Besides overall miniaturization and cost considerations, this extra length impacts the timing resolution [19].

Several scintillator–photosensor configurations can be considered [33]. In the most standard pixelated approach, each event is detected by a single detector. In an alternative configuration, scintillation light from one crystal is shared among a few photodetectors, improving the identification of the gamma ray position. When the read-out is based on monolithic crystal designs, or in the case of photosensors based on single-photon detection as for instance the digital photon counters [34], the information attached to each event is distributed on several channels, which can impact the timing resolution. Metascintillators challenge these traditional approaches. At the moment, we are developing prototypes in two directions, high-aspect ratio [35] quasimonolithic designs and metapixels.

In the following examples, we consider a pixelated array, with metascintillator pixels of size $3 \times 3 \times 27$ mm^3 and $3 \times 3 \times 35$ mm^3. These dimensions are chosen to correspond to the stopping power of an LYSO pixel of $3 \times 3 \times 20$ mm^3, for a plastic-based metascintillator with a CSV ratio of 0.5 and 1, respectively. Preliminary calculations of the Cramér–Rao lower bound have demonstrated a strong effect of energy sharing on the theoretical timing limit. For the configurations described above, the lower bound for detector time resolution is presented in Fig. 17. The bound calculation is mostly related to the availability of fast photons produced by the organic material, similar to [16]. The simulation was used to estimate the amount of detectable photons as a percentage of the produced ones, while the standard deviation of the time walk was taken into account as the stochastic factor.

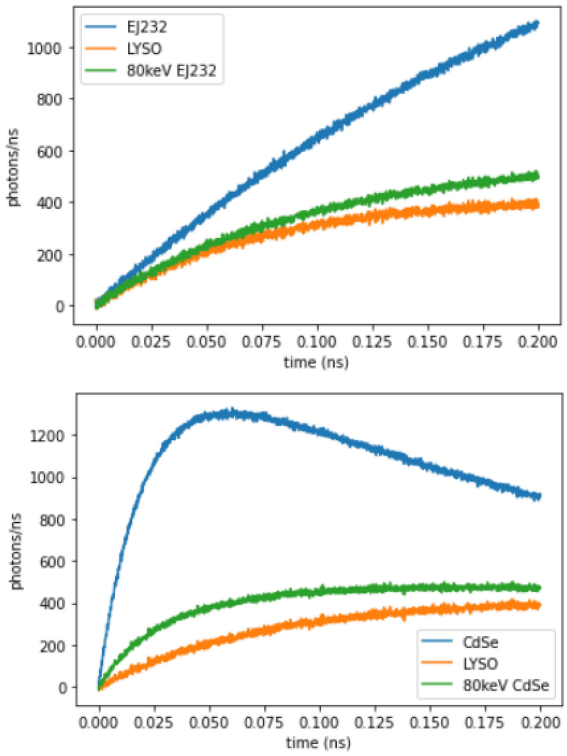

Fig. 16. First 200 ps from scintillation event onset for two different fast emitters (EJ232-top and CdSe-bottom) and three different energy sharing cases: 0, 80, and 511 keV deposited in the fast emitter. Lower light yield from CdSe is compensated by the extremely fast response, leading to a very discernable rising edge.

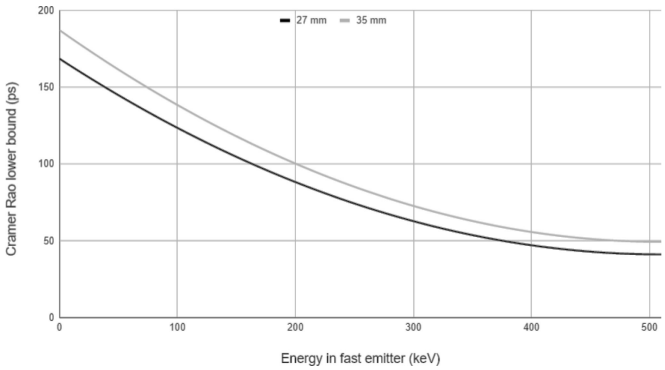

Fig. 17. Calculated lower timing bound for LYSO/EJ232 metascintillators of $3 \times 3 \times 27$ mm^3 and $3 \times 3 \times 35$ mm^3, relating the amount of an event's energy sharing [energy release in the fast emitter (keV)] to its expected timing resolution, for 511 keV events.

From the combination of this information and the probability distribution presented in Fig. 12, it is possible to create a distribution of timing resolution for the events resulting from each particular metascintillator configuration. In Fig. 18, we present the probability distribution corresponding to 27-mm pixel length and two different CSV ratios (1 and 0.5). From this calculation, we can quantify the timing characteristics of the metascintillator designs. For the pixel with ten pairs of layers (200-um LYSO and 100-um EJ232 thickness) and a final dimension of $3 \times 3 \times 27$ mm^3, this results in a weighted average timing resolution of 131.4 ps, whereas a purely LYSO event corresponds to 169.2 ps and an EJ232 event corresponds

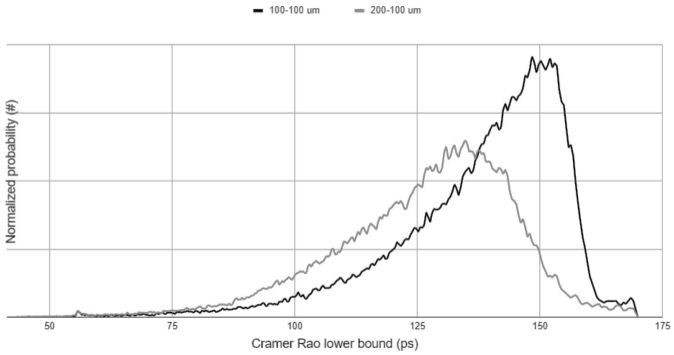

Fig. 18. Combination of the calculated lower bound of timing resolution and the energy sharing probability function, leading to a timing probability function for two different scenarios of metascintillators slab composition (100 LYSO-100 EJ232 μm and 200 LYSO-100 EJ232 μm) for a pixel of $3 \times 3 \times 27$ mm^3.

to 41.2 ps. The simple, plastic-based metascintillator demonstrates a weighted average value which improves the LYSO value by approximately 40 ps, and corresponds to approximately 30 ps better timing than an LYSO-alone pixel of the same stopping power. Furthermore, we must consider that in this distribution, a fraction of events has a significantly better CTR than the average value. These events can be used as priors in more elaborate image reconstruction algorithms than the ones in use today and help to constrain the other less precise events.

When this analysis is confirmed by experimental data, especially at the system level, the general concept of metascintillators will be able to demonstrate a novel, adaptable to new materials solution that breaks the detection efficiency–timing resolution tradeoff and can form the next paradigm, in the quest for the 10-ps CTR.

B. Cherenkov-Based Timing

The aforementioned approach on analyzing variable timing resolution of scintillation-based detectors is relevant for any type of detector where timing is different for each event. Another similar case corresponds to the detectors that base their timing characterization of individual events based on the existence of Cherenkov photons. While metascintillators use fast emitters for the faster production of photons, in Cherenkov-based detectors, Cherenkov light is emitted at the picosecond scale after ionization [36].

Cherenkov light is emitted in the deep blue-UV spectrum, depending on the refraction index of the material. Newly developed SiPMs for dark matter search experiments have the capability to retrieve this light with sufficiently high PDE. While this emission is low on intensity, leading to a few tens of photons in the best case, it is difficult to be used for energy or position characterization. Nevertheless, timing characterization is still possible. Indeed, the short emission time of Cerenkov photons (about 10 ps) allows very accurate figures of time resolution for a percentage of the recorded events, as a function of the number of photons detected.

Hybrid Cherenkov–scintillation detectors have been already proposed [37]. Moreover, Cherenkov detection is relevant to

the metascintillators in two ways. On the one hand, the stochastic variation of the number of produced and detected Cerenkov photons results in a distribution of timing resolution for the events recorded [38], in a similar way as for the metacrystals. On the other hand, metascintillators themselves, including various materials with various refractive indices, can be designed to provide Cherenkov of particular characteristics, which can provide better quality timing characterization. Such synergizing solution will be included of the metascintillators development program.

C. Future Developments

The optimal read-out approach for metascintillators has not yet been determined and this constitutes an active aspect of few investigations. While pixelated designs seem to demonstrate better timing, monolithic approaches, providing more statistics on light collection and determination of the impact depth of interaction component, could allow the development of tailored algorithms for metascintillators with significant advantages. Hybrid approaches of pseudo-pixelated designs can also be considered [39]. A very significant step in this direction is the combination of the unconventionally variable single-detector timing resolution with novel pulse identification approaches. As described in Fig. 7, there is a stochastic probability of each event in relation with its energy sharing content, information that can be measured and used to enhance the timing resolution of the detector. New research must be developed to include energy sharing to advanced algorithms [40]. Analytic expressions relating to the form of the light signal will be applied, and the possibility of using enhanced machine learning algorithms can further improve the quality on the timing of metascintillators [41].

A separate goal is to achieve, through the popularization of the concept and collaboration with system-level PET and scintillator development companies, a competitive cost for all of the above paradigms. At the same time, novel materials and methods, such as subsurface laser engraving processing [42] could find applications in the realm of metascintillators, leading to superior timing and improved cost effectiveness.

The ultimate goal of metascintillators is to achieve the development of a new set of PET image reconstruction approaches, based on the precise estimation of energy sharing and resulting variable event timing. An initial approach can simply divide events into timing groups, relating to their energy content, and use those in order to define a precise number of resolution elements, enhancing in this way the ToF-related sensitivity. Binning of the events can be directly driven by the dimensions of the examined subject or organ, drawing this way maximum information from variable timing. Moreover, using a fast set of events to guide reconstruction, through new mathematical tools such as sparse matrix analysis [43] or compressed sensing [44], is another exciting possibility.

The quest for the development of scintillation detectors with cutting-edge timing resolution is a multidisciplinary task, spanning several fields of science and technology. Metascintillators intend to provide a disruptive solution on the technological impasse created by the tradeoff between optical photon production and detection efficiency through a set of innovative approaches. We deem the metascintillator approach to be the foundation of future designs with novel materials, architectures, and read-out configurations, that have the potential to reach 10-ps CTR, as targeted by the 10-ps challenge [45].

The work is done in a spirit of openness and cooperation in order to enhance the scientific output and consequently provide technological solutions to the very important medical questions relating to PET applicability, for the advancement of public health.

D. Conclusion

Based on simulation results that confirm preliminary testing, a metascintillator can achieve significant effective timing improvement. As demonstrated for the BGO-plastic case [5], the energy sharing characteristic can be exploited to significantly enhance the single-detector timing resolution (Fig. 5). Our simulations and further investigation show that even in the simple scenario of combining LYSO with EJ232, single-detector effective timing resolution is improved by at least 30 ps compared to LYSO-alone, without deterioration in the gamma detection efficiency. This preliminary finding will be further expanded with experimental data. Nevertheless, existing proof-of-concept results already demonstrated the significant potential of metascintillators.

Novel designs, extending from the existing slab-sandwich geometry shown in Fig. 2, could lead to better statistical characteristics of energy sharing for lower CSV ratio and hence, higher effective stopping power. In the same context, the development of new scintillating materials, such as for instance organic–inorganic perovskites [17], can be used to adapt existing metascintillator topologies and further enhance their timing and stopping power characteristics. Research including CdSe nanoplatelets already shows very promising results, given their high photoelectric cross section and remarkable timing characteristics. Nevertheless, this approach has to overcome significant barriers relating to their deposition, orientation, and ways to avoid self-absorption.

Currently, we are broadening our simulation and analysis tools to also include nano-manufactured photonic materials within the metascintillator ensemble: another stochastic process related to light guiding. However, this expansion will lead to a general unified model of scintillation, connecting light production, and photoelectric cross section characteristics of the constituting materials, to a precise estimation of light collection and timing characteristics. This will allow further investigation with new materials and arrangements.

ACKNOWLEDGMENT

The authors would like to thank the team members of their labs for having contributed in the described projects and investigations through their multiple efforts. In particular, the authors would like to thank Laura Moliner Martinez for her work on energy sharing simulations and Gabriel Cañizares Ledo for simulations on optical propagation.

REFERENCES

[1] *Healthcare Resource Statistics—Technical Resources and Medical Technology, Availability of Technical Resources in Hospitals*, Eurostat, Luxembourg City, Luxembourg, Aug. 2020.

[2] D. L. Bailey, S. R. Meikle, and T. Jones, "Effective sensitivity in 3D PET: The impact of detector dead time on 3D system performance," *IEEE Trans. Nucl. Sci.*, vol. 44, no. 3, pp. 1180–1185, Jun. 1997.

[3] S. R. Cherry, T. Jones, J. S. Karp, J. Qi, W. Moses, and R. D. Badawi, "Total-body PET: Maximizing sensitivity to create new opportunities for clinical research and patient care," *J. Nucl. Med.*, vol. 59, no. 1, pp. 3–12, 2018.

[4] S. Surti, "Update on time-of-flight PET imaging," *J. Nucl. Med.*, vol. 56, no. 1, pp. 98–105, 2015.

[5] T. F. Budinger, "Time-of-flight positron emission tomography: Status relative to conventional PET," *J. Nucl. Med.*, vol. 24, no. 1, pp. 73–78, 1983.

[6] J. van Sluis *et al.*, "Performance characteristics of the digital biograph vision PET/CT system," *J. Nucl. Med.*, vol. 60, no. 7, pp. 1031–1036, 2019.

[7] A. Del Guerra, N. Belcari, and M. Bisogni, "Positron emission tomography: Its 65 years," *La Rivista del Nuovo Cimento*, vol. 39, no. 4, pp. 155–223, 2016.

[8] P. Lecoq *et al.*, "Roadmap toward the 10 ps time-of-flight PET challenge", *Phys. Med. Biol.*, vol. 65, no. 21, 2020, Art. no. 21RM01.

[9] I. Shiri, H. Abdollahi, M. R. Atashzar, A. Rahmim, and H. Zaidi, "A theranostic approach based on radiolabeled antiviral drugs, antibodies and CRISPR-associated proteins for early detection and treatment of SARS-CoV-2 disease," *Nucl. Med. Commun.*, vol. 41, no. 9, pp. 837–840, 2020.

[10] C. Betancourt, A, Dätwyler, P. Owen, A. Puig, and N. Serra, "SiPM single photon time resolution measured via bi-luminescence," *Nucl. Instrum. Methods Phys. Res. A Accelerators Spectrometers Detectors Assoc. Equip.*, vol. 958, Apr. 2020, Art. no. 162851.

[11] F. Nolet *et al.*, "22 μW, 5.1 ps LSB, 5.5 ps RMS jitter Vernier time-to-digital converter in CMOS 65 nm for single photon avalanche diode array," *Electron. Lett.*, vol. 56, no. 9, pp. 424–426, 2020.

[12] P. Lecoq, A. Gektin, and M. Korzhik, "Scintillation and inorganic scintillators," in *Inorganic Scintillators for Detector Systems. Particle Acceleration and Detection*. Cham, Switzerland: Springer, 2017.

[13] W. S. Choong, "The timing resolution of scintillation-detector systems: Monte Carlo analysis," *Phys. Med. Biol.*, vol. 54, no. 21, p. 6495, 2009.

[14] C. Pepin *et al.*, "Properties of LYSO and recent LSO scintillators for phoswich PET detectors," *IEEE Trans. Nucl. Sci.*, vol. 51, no. 3, pp. 789–795, Jun. 2004.

[15] R. Y. Zhu, "Ultrafast and radiation hard inorganic scintillators for future HEP experiments," *J. Phys. Conf. Series*, vol. 1162, no. 1, Jan. 2019, Art. no. 012022.

[16] X. Wen and J. P. Hayward, "Time resolution measurements of EJ-232Q with single and dual-sided readouts," *IEEE Trans. Nucl. Sci.*, vol. 67, no. 6, pp. 2081–2088, Sep. 2020.

[17] P. Moskal *et al.*, "Time resolution of the plastic scintillator strips with matrix photomultiplier readout for J-PET tomograph," *Phys. Med. Biol.*, vol. 61, no. 5, pp. 2025–2047, 2025.

[18] V. B. Mykhaylyk, H. Kraus, and M. Saliba, "Bright and fast scintillation of organolead perovskite MAPbBr 3 at low temperatures," *Mater. Horizons*, vol. 6, no. 8, pp. 1740–1747, 2019.

[19] J. W. Cates and C. S. Levin, "Advances in coincidence time resolution for PET," *Phys. Med. Biol.*, vol. 61, no. 6, p. 2255, 2016.

[20] S. Seifert, H. T. van Dam, and D. R. Schaart, "The lower bound on the timing resolution of scintillation detectors," *Phys. Med. Biol.*, vol. 57, no. 7, p. 1797, 2012.

[21] R. S. Kshetrimayum, "A brief intro to metamaterials," *IEEE Potentials*, vol. 23, no. 5, pp. 44–46, Jan. 2005.

[22] *Lexico*. Accessed: Aug. 19, 2020. [Online]. Available: https://www.lexico.com/definition/metamaterial

[23] P. Lecoq, "Pushing the limits in time-of-flight PET imaging," *IEEE Trans. Radiat. Plasma Med. Sci.*, vol. 1, no. 6, pp. 473–485, Nov. 2017.

[24] R. M. Turtos, S. Gundacker, E. Auffray, and P. Lecoq, "Towards a metamaterial approach for fast timing in PET: Experimental proof-of-concept," *Phys. Med. Biol.*, vol. 64, no. 18, 2019, Art. no. 185018.

[25] S. Gundacker *et al.*, "Experimental time resolution limits of modern SiPMs and TOF-PET detectors exploring different scintillators and Cherenkov emission," *Phys. Med. Biol.*, vol. 65, no. 2, 2020, Art. no. 025001.

[26] R. M. Turtos *et al.*, "On the use of CdSe scintillating nanoplatelets as time taggers for high-energy gamma detection," *NPJ 2D Mater. Appl.*, vol. 3, p. 37, Oct. 2019. [Online]. Available: https://doi.org/10.1038/s41699-019-0120-8

[27] P. Lecoq, "Metamaterials for novel X- or g-ray detector designs," in *Proc. IEEE Nucl. Sci. Symp. Conf. Rec.*, 2009, pp. 680–684.

[28] M. Kronberger, E. Auffray, and P. R. Lecoq, "Improving light extraction from heavy inorganic scintillators by photonic crystals," *IEEE Trans. Nucl. Sci.*, vol. 57, no. 5, pp. 2475–2482, Oct. 2010.

[29] M. Salomoni, R. Pots, E. Auffray, and P. Lecoq, "Enhancing light extraction of inorganic scintillators using photonic crystals," *Crystals*, vol. 8, no. 2, p. 78, 2018.

[30] M. Salomoni *et al.*, "Photonic crystal slabs applied to inorganic scintillators," *IEEE Trans. Nucl. Sci.*, vol. 65, no. 8, pp. 2191–2195, Aug. 2018.

[31] G. Konstantino *et al.*, "A novel metascintillator approach for ultra-fast timing in positron emission tomography," in *Proc. IEEE Nucl. Sci. Symp. Med. Imag. Conf. (NSS/MIC)*, 2020, pp. 1–4.

[32] S. Jan *et al.*, "GATE: A simulation toolkit for PET and SPECT," *Phys. Med. Biol.*, vol. 49, no. 19, pp. 4543–4561, 2004.

[33] E. Lamprou, A. J. Gonzalez, F. Sanchez, and J. M. Benlloch, "Exploring TOF capabilities of PET detector blocks based on large monolithic crystals and analog SiPMs," *Physica Medica*, vol. 70, pp. 10–18, Feb. 2020.

[34] S. E. Brunner, L. Gruber, A. Hirtl, K. Suzuki, J. Marton, and D. R. Schaart, "A comprehensive characterization of the time resolution of the Philips digital photon counter," *J. Instrument.*, vol. 11, no. 11, 2016, Art. no. P11004.

[35] J. Barrio, N. Cucarella, A. J. Gonzalez, M. Freire, V. Ilisie, and J. M. Benlloch, "Characterization of a high aspect ratio detector with lateral sides readout for Compton PET," *IEEE Trans. Radiat. Plasma Med. Sci.*, vol. 4, no. 5, pp. 546–554, Sep. 2020.

[36] J. Caravaca, F. B. Descamps, B. J. Land, M. Yeh, and G. O. Gann, "Cherenkov and scintillation light separation in organic liquid scintillators," *Eur. Phys. J. C*, vol. 77, no. 12, pp. 1–7, 2017.

[37] S. E. Brunner and D. R. Schaart, "BGO as a hybrid scintillator/Cherenkov radiator for cost-effective time-of-flight PET," *Phys. Med. Biol.*, vol. 62, no. 11, p. 4421, 2017.

[38] N. Efthimiou *et al.*, "TOF-PET image reconstruction with multiple timing kernels applied on Cherenkov radiation in BGO," *IEEE Trans. Radiat. Plasma Med. Sci.*, early access, Dec. 31, 2020, doi: 10.1109/TRPMS.2020.3048642.

[39] J. V. Panetta, S. Surti, B. Singh, and J. S. Karp, "Characterization of monolithic scintillation detectors etched witsh laser induced optical barriers," *IEEE Trans. Radiat. Plasma Med. Sci.*, vol. 3, no. 5, pp. 531–537, Sep. 2019.

[40] S. Xie, X. Zhang, Q. Huang, Z. Gong, J. Xu, and Q. Peng, "Methods to compensate the time walk errors in timing measurements for PET detectors," *IEEE Trans. Radiat. Plasma Med. Sci.*, vol. 4, no. 5, pp. 555–562, Sep. 2020, doi: 10.1109/TRPMS.2020.2981388.

[41] A. J. Gonzalez, J. Barrio, E. Lamprou, V. Ilisie, F. Sanchez, and J. M. Benlloch, "Progress reports on the MEDAMI 2019 and CTR research at the DMIL in i3M," *IL Nuovo Cimento*, vol. 100, no. 5, p. 43, 2020.

[42] G. Konstantinou, R. Chil, M. Desco, and J. J. Vaquero, "Subsurface laser engraving techniques for scintillator crystals: Methods, applications, and advantages," *IEEE Trans. Radiat. Plasma Med. Sci.*, vol. 1, no. 5, pp. 377–384, Sep. 2017.

[43] J. Zhou and J. Qi, "Fast and efficient fully 3D PET image reconstruction using sparse system matrix factorization with GPU acceleration," *Phys. Med. Biol.*, vol. 56, no. 20, p. 6739, 2011.

[44] K. Malczewski, "PET image reconstruction using compressed sensing," in *Proc. IEEE Signal Process. Algorithms, Architect. Arrangements Appl. (SPA)*, Sep. 2013, pp. 176–181.

[45] P. Lecoq, C. Morel, and J. Prior. *The10ps-Challenge*. Accessed: Aug. 19, 2020. [Online]. Available: https://the10ps-challenge.org